

# Excitonic polaritons in Fibonacci quasicrystals

J. Hendrickson<sup>1\*</sup>, B. C. Richards<sup>1</sup>, J. Sweet<sup>1</sup>, G. Khitrova<sup>1</sup>, A. N. Poddubny<sup>2</sup>,  
E. L. Ivchenko<sup>2</sup>, M. Wegener<sup>3</sup>, and H. M. Gibbs<sup>1</sup>

<sup>1</sup>College of Optical Sciences, The University of Arizona, Tucson, AZ 85721

<sup>2</sup>A. F. Ioffe Physico-Technical Institute, 194021 St. Petersburg, Russia

<sup>3</sup>Institut für Angewandte Physik, Universität Karlsruhe (TH)

Wolfgang-Gaede-Strasse 1, D-76131 Karlsruhe, Germany

\*Corresponding Author: [jhendrickson@optics.arizona.edu](mailto:jhendrickson@optics.arizona.edu)

**Abstract:** The fabrication and characterization of light-emitting one-dimensional photonic quasicrystals based on excitonic resonances is reported. The structures consist of high-quality GaAs/AlGaAs quantum wells grown by molecular-beam epitaxy with wavelength-scale spacings satisfying a Fibonacci sequence. The polaritonic (resonant light-matter coupling) effects and light emission originate from the quantum well excitonic resonances. Measured reflectivity spectra as a function of detuning between emission and Bragg wavelength are in good agreement with excitonic polariton theory. Photoluminescence experiments show that active photonic quasicrystals, unlike photonic crystals, can be good light emitters: While their long-range order results in a stopband similar to that of photonic crystals, the lack of periodicity results in strong emission.

©2008 Optical Society of America

**OCIS codes:** (160.5293) Photonic bandgap materials; (230.5590) Quantum-well, -wire and -dot devices

---

## References and links

1. D. Shechtman, I. Blech, D. Gratias, J. W. Cahn, "Metallic phase with long-range orientational order and no translational symmetry," *Phys. Rev. Lett.* **53**, 1951–1953 (1984).
2. C. Janot, *Quasicrystals* (Clarendon Press, Oxford, 1994).
3. A. Ledermann et al, "Three-dimensional silicon inverse photonic quasicrystals for infrared wavelengths," *Nat. Mater.* **5**, 942-945 (2006).
4. W. Man, M. Megens, P. J. Steinhardt, P. M. Chaikin, "Experimental measurement of the photonic properties of icosahedral quasicrystals," *Nature* **436**, 993-996 (2005).
5. B. Freedman et al, "Wave and defect dynamics in nonlinear photonic quasicrystals," *Nature* **440**, 1166-1169 (2006).
6. M. A. Kaliteevski et al, "Diffraction and transmission of light in low-refractive index Penrose-tiled photonic quasicrystals," *J. Phys.: Condens. Matter* **13**, 10459-10470 (2001).
7. R. Merlin, K. Bajema, R. Clarke, F.-Y. Juang, P. K. Bhattacharya, "Quasiperiodic GaAs-AlAs heterostructures," *Phys. Rev. Lett.* **55**, 1768-1770 (1985).
8. F. Laruelle and B. Etienne, "Fibonacci invariant and electronic properties of GaAs/Ga<sub>1-x</sub>Al<sub>x</sub>As quasiperiodic superlattices," *Phys. Rev. B* **37**, 4816-4819 (1988).
9. W. Gellermann, M. Kohmoto, B. Sutherland, P. C. Taylor, "Localization of light waves in Fibonacci dielectric multilayers," *Phys. Rev. Lett.* **72**, 633-636 (1994).
10. N. Liu, "Propagation of light waves in Thue-Morse dielectric multilayers," *Phys. Rev. B* **55**, 3543-3547 (1997).
11. R. W. Peng et al, "Symmetry-induced perfect transmission of light waves in quasiperiodic dielectric multilayers," *Appl. Phys. Lett.* **80**, 3063-3065 (2002).
12. L. Dal Negro et al, "Light transport through the band-edge states of Fibonacci quasicrystals," *Phys. Rev. Lett.* **90**, 055501 (2003).
13. L. Dal Negro et al., "Photon band gap properties and omnidirectional reflectance in Si/SiO<sub>2</sub> Thue-Morse quasicrystals," *Appl. Phys. Lett.* **84**, 5186-5188 (2004).
14. T. Hattori, N. Tsurumachi, S. Kawato, H. Nakatsuka, "Photonic dispersion relation in a one-dimensional quasicrystal," *Phys. Rev. B* **50**, 4220-4223 (1994).
15. M. A. Kaliteevski, V. V. Nikolaev, R. A. Abram, S. Brand, "Bandgap structures of optical Fibonacci lattices after light diffraction," *Opt. Spectrosc.* **91**, 109-118 (2001).

16. L. Dal Negro et al., "Spectrally enhanced light emission from aperiodic photonic structures," *Appl. Phys. Lett.* **86**, 261905 (2005).
17. K. Nozaki and T. Baba, "Quasiperiodic photonic crystal microcavity lasers," *Appl. Phys. Lett.* **84**, 4875-4877 (2004).
18. S.-K. Kim, J.-H. Lee, S.-H. Kim, I.-K. Hwang, Y. H. Lee, "Photonic quasicrystal single-cell cavity mode," *Appl. Phys. Lett.* **86**, 031101 (2005).
19. E. L. Albuquerque and M. G. Cottam, "Theory of elementary excitations in quasiperiodic structures," *Phys. Reports* **376**, 225-337 (2003).
20. M. S. Vasconcelos, P. W. Mauriz, F. F. de Medeiros, E. L. Albuquerque, "Photonic band gaps in quasiperiodic photonic crystals with negative refractive index," *Phys. Rev. B* **76**, 165117 (2007).
21. S. V. Gaponenko, S. V. Zhukovsky, A. V. Lavrinenko, K. S. Sandomirskii, "Propagation of waves in layered structures viewed as number recognition," *Optics Commun.* **205**, 49-57 (2002).
22. M. S. Vasconcelos, E. L. Albuquerque, A. M. Mariz, "Optical localization in quasi-periodic multilayers," *J. Phys. Cond. Mat.* **10**, 5839-5849 (1998).
23. E. M. Nascimento, F. A. B. F. de Moura, M. L. Lyra, "Scaling laws for the transmission of random binary dielectric multilayered structures," *Phys. Rev. B* **76**, 115120 (2007).
24. M. S. Vasconcelos and E. L. Albuquerque, "Plasmon-polariton fractal spectra in quasiperiodic multilayers," *Phys. Rev. B* **57**, 2826-2833 (1998).
25. E. L. Albuquerque and M. G. Cottam, *Polaritons in Periodic and Quasiperiodic Structures* (Elsevier, Amsterdam, The Netherlands, 2004).
26. E. L. Ivchenko, "Excitonic polaritons in periodic quantum-well structures," *Sov. Phys. Solid State* **33**, 1344-1349 (1991).
27. E. L. Ivchenko, A. I. Nesvizhskii, S. Jorda, "Bragg reflection of light from quantum-well structures," *Phys. Sol. Stat.* **36**, 1156-1161 (1994).
28. E. L. Ivchenko, *Optical Spectroscopy of Semiconductor Nanostructures* (Alpha Science International, Harrow, U. K., 2005).
29. M. Hübner et al., "Optical lattices achieved by excitons in periodic quantum well structures," *Phys. Rev. Lett.* **83**, 2841-2844 (1999).
30. J. P. Prineas et al., "Exciton-polariton eigenmodes in light-coupled  $\text{In}_{0.04}\text{Ga}_{0.96}\text{As}/\text{GaAs}$  semiconductor multiple-quantum-well periodic structures," *Phys. Rev. B* **61**, 13863-13872 (2000).
31. A. N. Poddubny, L. Pillozzi, M. M. Voronov, E. L. Ivchenko, "Resonant Fibonacci quantum well structures in one dimension," *Phys. Rev. B* **77**, 113306 (2008).
32. V. P. Kochereshko et al., "Giant exciton resonance reflectance in Bragg MQW structures," *Superlatt. Microstruct.* Vol. **15**, No. 4, 471-473 (1994).
33. L. I. Deych, M. V. Erementchouk, A. A. Lisyansky, E. L. Ivchenko, M. M. Voronov, "Exciton luminescence in one-dimensional resonant photonic crystals: A phenomenological approach," *Phys. Rev. B* **76**, 075350 (2007).

When Italian mathematician Leonardo da Pisa, called Fibonacci (1180-1240), came up with his now famous sequence of numbers, it is not likely that he foresaw either quasicrystals or the impact that quasicrystals would one day have as a new form of matter. Quasicrystals are nonperiodic, yet they exhibit long-range order resulting from the underlying deterministic construction principle [1,2]. In recent years, man-made quasicrystals with inter-atomic spacings comparable to the wavelength of light, "photonic quasicrystals", have become available even in three dimensions [3-6]; so far these structures have been passive, i.e., they do not emit light. In one dimension (1D), the Fibonacci sequence can be directly translated into a layered quasicrystal structure (Fig. 1), which is amenable to atomic-precision growth via molecular-beam epitaxy (MBE). Fibonacci-spaced semiconductor multilayer structures have been grown and studied before; they differ from the present photonic structures by having very thin layers for electron wavefunction interferences [7,8]. 1D passive photonic quasicrystals and aperiodic structures have also been realized some years ago [9-15]; they involve nonresonant dielectrics, quite different from the excitonic resonances studied here. Active aperiodic Thue-Morse multilayer one-dimensional structures of nonresonant dielectrics ( $\text{SiN}_x/\text{SiO}_2$ ) have been fabricated with enhanced emission compared with homogeneous  $\text{SiN}_x$  dielectrics [16]. Quasicrystal lasers have also been reported [17,18]; these utilize a 2D photonic quasicrystal slab. Highly localized modes occur when a few holes are omitted, very much as for photonic crystal lasers; in contrast the eigenmodes of our photonic quasicrystals are delocalized. Unlike photonic crystal slabs, lasing was also seen with no missing holes in an extended but partly localized mode at the photonic gap edge [17].

We chose to study the Fibonacci sequence because it is the most well-known example of 1D quasiperiodic structures, along with Thue-Morse structures and the Cantor structure [13,16,19-25]; its distinctive feature is a dense quasi-continuous pure point Fourier spectrum [19,2]. Another interesting property of Fibonacci structures is their direct connection with the 2D and 3D quasicrystals, the Penrose lattices [2,3].

To allow for a well-defined reference point for the novel active 1D *quasicrystalline* structures to be discussed below, we first briefly review the well-known yet appealing physics of a *crystalline* arrangement of  $N$  optically active QWs, periodically spaced by half the exciton wavelength  $\lambda$  in the material (typically,  $N > 10$  is sufficient), so that the period of the structure  $d$  equals the Bragg value  $d_{\text{Bragg}} \equiv \lambda/2 = \lambda_0/2n$ , where  $\lambda_0$  is the vacuum wavelength, and  $n$  is the effective refractive index of the materials between the QW centers. In this periodic case, the coupling of the  $N$  QWs via the electromagnetic field lifts the  $N$ -fold degeneracy in a particular manner: While  $(N-1)$  subradiant modes experience only very little coupling to the field, most of the oscillator strength is concentrated in a single superradiant mode [26-30]. Approximately, the radiative damping of this superradiant mode increases proportional to  $N$ . This increase makes competing nonradiative dephasing channels (e.g., disorder or phonon damping) irrelevant for large enough  $N$ . At first sight, this enhanced light-matter coupling appears to be ideal for an efficient light-emitting structure. Yet, it is not. For

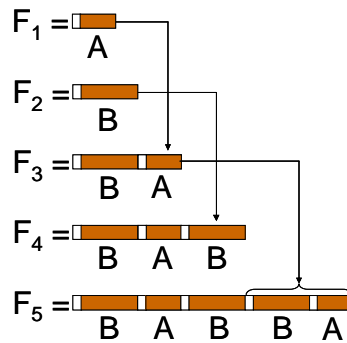


Fig. 1. An active quasicrystal of quantum wells. A QW Fibonacci chain has two distances containing a QW: a small distance A and a large distance B.  $F_{j+1}$  is formed by adding  $F_{j-1}$  to the end of  $F_j$ : BABBABABBABBA....

the exact Bragg condition and for emission normal to the layers of the Bragg stack, the corresponding standing wave pattern has nodes at the QW positions in real space – obviously leading to inefficient emission in this direction. Correspondingly, in the frequency domain, the emission wavelength lies within the photonic crystal stopband. We will see that these unfavorable conditions no longer exist in 1D quasicrystalline structures where the Bragg condition can be effectively maintained, yet not all of the QWs are located at field-node positions.

Such a 1D quasicrystal is illustrated in Fig. 1; the Fibonacci chain  $F_j$  contains QWs with two different separations A and B between the centers of the wells. The ratio of the optical pathlengths of B to A equals the golden mean  $(\sqrt{5} + 1)/2$ ; the Fibonacci recursion is illustrated in Fig. 1. We chose the well established GaAs/AlGaAs material as a model system. The Bragg condition for the Fibonacci structure of the smallest possible thickness can be presented in the same form as for the periodic one,  $\bar{d} = d_{\text{Bragg}}$ , where  $\bar{d} = (5-\sqrt{5})A/2$  stands for the mean period of the lattice, and  $d_{\text{Bragg}} = \lambda/2$  [31]. The Fibonacci Bragg resonance results in a superradiant mode with the radiative rate  $\eta N \Gamma_0$ , where  $\eta$  is close to unity and  $\Gamma_0$  is the radiative decay rate of a single QW. Frequencies of the other  $(N-1)$  modes have much smaller

but nonzero imaginary parts. These weakly radiating modes contribute to the fine structure of the reflection spectrum in the vicinity of the exciton resonance frequency as shown below.

The QW samples were grown by molecular beam epitaxy on (001), zero-degree-cut GaAs substrates. Each GaAs QW (nominally 22 nm thick) was grown between 5-nm-thick  $\text{Al}_{0.3}\text{Ga}_{0.7}\text{As}$  barriers. The target lengths  $L_A$  and  $L_B$  for A and B of a Fibonacci chain sample were then reached by growing  $\text{Al}_{0.04}\text{Ga}_{0.96}\text{As}$  superlattices. The physical thicknesses of A and B are roughly 82 and 134 nm for the Bragg condition; the ratio of their optical thicknesses is the golden mean value. The optical thickness of A is  $d_{\text{QW}}n_{\text{QW}} + (L_A - d_{\text{QW}})n_{\text{barrier}}$ , where  $d_{\text{QW}}$  is the thickness of the QW; here the QW background index  $n_{\text{QW}}$  is almost the same as  $n_{\text{barrier}}$ . The samples were not anti-reflection coated; for the Bragg condition, the optical thickness from the vacuum interface to the center of the first QW is  $\lambda/2$ .

The sample was placed in a continuous-flow helium cryostat with internal nanopositioners. For photoluminescence (PL) measurements, the sample was pumped above band by emission at 780 nm from a continuous-wave Titanium-sapphire ring laser. For a reflectivity measurement, the sample was probed by the emission from a broad band tungsten lamp spectrally filtered by an interference filter (FWHM 10 nm) centered at the wavelength of the heavy hole. A reflecting microscope objective (NA = 0.5) was used to focus the excitation beam onto the sample with a 1  $\mu\text{m}$  spot size and to subsequently collect the PL or reflected signal in reflection geometry. The signal was then dispersed by a spectrometer and detected on a 2D silicon CCD array camera using a 0.1 s acquisition time. The spectral resolution of this apparatus was 0.2  $\text{\AA}$ . The reflectivity data were normalized using a highly reflective distributed-Bragg-reflector (DBR) sample placed in the cryostat adjacent to the Fibonacci sample.

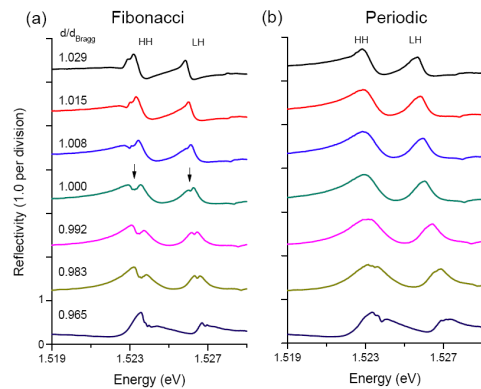


Fig. 2. Comparison of the thickness dependence of the reflectivity. The spacing of the 21 QWs is either (a) a Fibonacci sequence with *optical* thicknesses (at Bragg) of  $A = 0.36\lambda_0$  and  $B = 0.59\lambda_0$  or (b) equidistant at  $\lambda_0/2$ . A reflectivity dip is present at the Bragg resonance only in (a), indicating the larger absorption. Each curve of larger  $d/d_{\text{Bragg}}$  is shifted up by one unit of reflectivity from the preceding one.

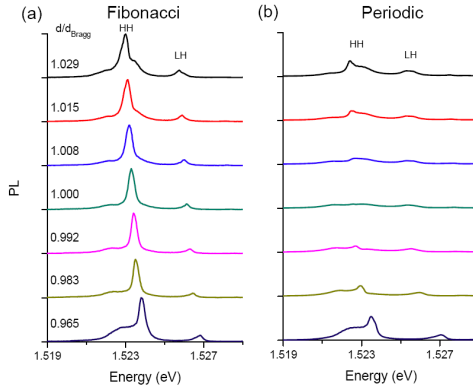


Fig. 3. Comparison of photoluminescence intensities. Conditions are the same as Fig. 2 with weak excitation at 1.59 eV. The PL from light holes is weak because of their rapid relaxation. The PL is strong at Bragg only in the Fibonacci case. All PL spectra have the same vertical scale, so relative comparisons are meaningful. Equal vertical shifts separate the spectra of different  $d/d_{\text{Bragg}}$ .

We grew and measured the reflectivity of Fibonacci QW samples with  $N = 21$  (sample FIB12) and 54 (FIB13) as well as a periodically spaced sample with  $N = 21$  (FIB14). Figure 2 compares the reflectivity for the two samples with  $N = 21$ . A reflectivity maximum with broad linewidth occurs at the Bragg condition for both samples for both the heavy-hole (HH) and the light-hole (LH) resonances. This maximum is just the well known photonic stopband, which is in agreement with previous work on active 1D photonic crystals using excitonic resonances in QWs of other materials [32,30]. Notably, however, the stop band is smooth for

the crystalline structure, whereas it reveals a pronounced fine structure (dips, see arrows) for the Fibonacci quasicrystals. This fine structure is visible for both the heavy- and the light-hole exciton resonances – strongly suggesting that this signature is a fingerprint of the quasicrystal. Indeed, recent theoretical work on active 1D Fibonacci quasicrystals utilizing excitonic resonances has predicted such fine structure [31].

One expects enhanced light-matter coupling for the frequencies corresponding to dips in reflectivity, so we have performed additional PL experiments. We excite the structures off-resonantly at low temperatures and detect the PL emerging from the sample normal to the sample surface. Figure 3 shows corresponding results. Periodic structures are shown as well in order to allow for a direct comparison. The behavior is very different for the periodic and the quasiperiodic structures. For the reference periodic structure, the PL almost vanishes for the Bragg condition – because every QW is at a node of the field. In sharp contrast to this, the PL for the Fibonacci quasicrystal at around the effective Bragg condition is still strong and quite narrow. This PL is spectrally centered at the dips in reflectivity (Fig. 2); this aspect is particularly clear for the  $N = 54$  QW sample, as shown in Fig. 4.

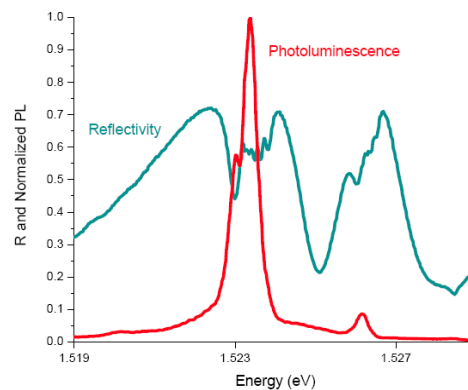


Fig. 4. PL and reflectivity of QW Fibonacci chain. The optical thicknesses (at Bragg) are  $A = 0.36\lambda_0$  and  $B = 0.59\lambda_0$ ;  $N = 54$ . The PL HH and LH peaks coincide with the dips in reflectivity.

So far, we have focused our discussion of the PL data on the resonant and low-excitation case. As a function of detuning from the Bragg thickness, the emission becomes more complex due to light-matter coupling interferences, as was shown for periodic QWs [30,33]. With increasing excitation level and hence higher carrier densities (not shown), the excitonic resonances are broadened, resulting in less structured PL spectra. Because of excitonic nonlinearities the polaritonic effects leading to the reflectivity dips are reduced as the excitation level is increased.

Finally, we compare the experiment to the recently developed theory of 1D active Fibonacci quasicrystals utilizing excitonic polaritons [31]. Here, the optical spectra are calculated based on a transfer-matrix approach, with parameters corresponding to our experiments. Clearly, the choice of the appropriate optical susceptibility  $\chi(\omega)$  of an individual QW is crucial. Thus, we start by fitting the reflectivity of a *single* QW to experiment (Fig. 5(a) & (b)) using a Lorentzian form:  $\chi(\omega) = \Gamma_{0HH}/(\omega_{HH} - \omega - i\Gamma_{HH}) + \Gamma_{0LH}/(\omega_{LH} - \omega - i\Gamma_{LH})$ , where  $\omega_{HH}$  is the radial frequency of the resonance,  $\Gamma_{0HH}$  is the radiative HWHM linewidth, and  $\Gamma_{HH}$  is the nonradiative HWHM of the heavy hole, etc. Next, this susceptibility is used for calculating the optical spectra of the Fibonacci structure FIB13 ( $N = 54$ ) in Fig. 5(d). Given the complexity of the optical spectra and the simplicity of the assumed susceptibility, the agreement has to be considered as very good. In particular, this comparison gives us additional confidence that the discussed fine structure in the optical spectra is actually due to

the 1D Fibonacci photonic quasicrystal. That the field overlap with QWs is much better for the Fibonacci spacings than for periodic is shown in Fig. 6; this explains the much stronger PL in the Fibonacci case.

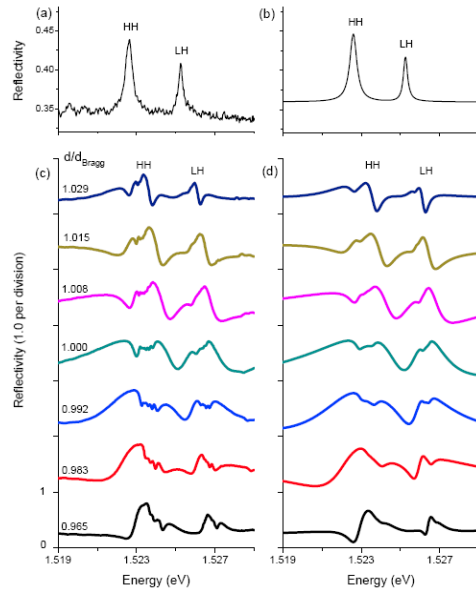


Fig. 5. Comparison between reflectivity measurements and transfer matrix computations. (a) Measured reflectivity for an uncoated GaAs/AlGaAs QW half a wavelength beneath the GaAs/vacuum interface (sample FIB10). (b) Corresponding computed reflectivity with the QW susceptibility approximated by Lorentzians with the following parameters: for the heavy hole, nonradiative half width  $\Gamma_{\text{HH}} = 180 \mu\text{eV}$  and radiative width  $\Gamma_{\text{0HH}} = 25 \mu\text{eV}$ ; for the light hole,  $\Gamma_{\text{LH}} = 115 \mu\text{eV}$  and  $\Gamma_{\text{0LH}} = 10 \mu\text{eV}$ . (c) Measured reflectivity for a 54 QW Fibonacci chain versus layer thickness. (d) Corresponding computed reflectivity using the same parameters as in (a). In (c) and (d) each curve of larger  $d/d_{\text{Bragg}}$  is shifted up by one unit of reflectivity from the preceding one. The vertical scales and  $d/d_{\text{Bragg}}$  values are the same for the data and computations.

In conclusion, we have fabricated active one-dimensional Fibonacci photonic quasicrystals using the excitonic resonance of high-quality GaAs/AlGaAs quantum wells. The quasicrystal long-range order results in an excitonic polariton stopband similar to that of photonic crystals. Yet, the lack of periodicity in the quasicrystal results in efficient photoluminescence emission in the direction normal to the layer planes, unlike the crystalline case.

### Acknowledgments

We thank D. Gerthsen and D. Litvinov for helpful discussions. The Tucson group thanks AFOSR, NSF, and JSOP for support. The St. Petersburg work was supported by RFBR and the “Dynasty” Foundation – ICFPM. The group of M.W. acknowledges financial support provided by the Deutsche Forschungsgemeinschaft (DFG) and the State of Baden-Württemberg through the DFG-Center for Functional Nanostructures (CFN) within subproject A1.4.

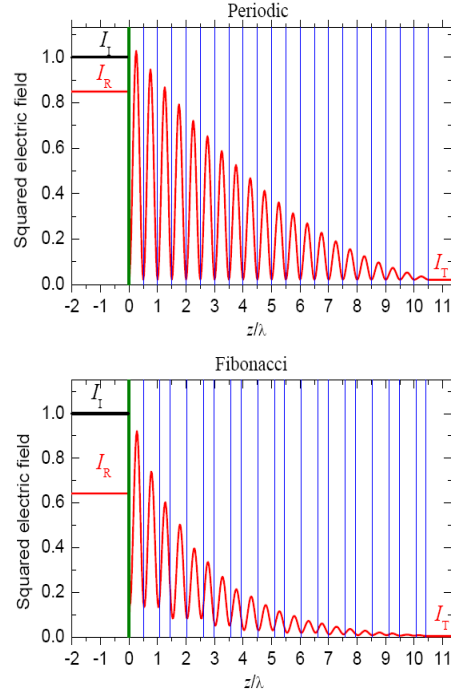


Fig. 6. Calculated distribution of the squared electric field in the periodic (a) and Fibonacci (b) QW structures with 21 wells with a plane wave incident from the left (at the HH exciton resonance frequency and for the Bragg condition). The thin blue lines indicate the QW positions while the green line separates the vacuum region from the sample. Values of  $|E_0|^2$  for  $z > 0$  were multiplied by the background refractive index  $n_{\text{barrier}} = 3.59$  for a better presentation. The incident, reflected, and transmitted waves are shown by horizontal lines  $I_i$ ,  $I_r$ , and  $I_t$ .